Arabian Journal of Chemistry (2021) **14**, 103117

King Saud University

Arabian Journal of Chemistry

www.ksu.edu.sa
www.sciencedirect.com

ORIGINAL ARTICLE

Synthesis, crystal structure and anticancer activities of an unusual inorganic–organic hybrid complex with a sandwiched ribbon structure

Jing Hu [a], Jiajia Qi [a], Yun Luo [a], Tianyue Yin [a], Jie Wang [a], Chunjing Wang [b], Wenge Li [a,*], Lili Liang [a,*]

[a] *Department of Chemistry, Bengbu Medical College, Donghai Avenue, Bengbu 233030, Anhui, China*
[b] *Department of Biological Sciences, Bengbu Medical College, Donghai Avenue, Bengbu 233030, Anhui, China*

Received 12 January 2021; accepted 8 March 2021
Available online 21 March 2021

KEYWORDS

Heptanuclear Cadmium complex;
4-Aminoantipyrine;
Sandwiched ribbon;
Antitumor activity

Abstract An inorganic-organic hybrid complex $[Cd_7Cl_{14}L_2(EtOH)_2]n$ (L = 4-Aminoantipyrine) was synthesised by solvothermal reaction and characterised by X-ray single-crystal diffraction analyses. It has unusual seven-nuclear cadmium chloride structure, which extends along the a-axis to form an infinite flat ribbon structure with the thickness of 3 Å and the width of 18 Å. The flat inorganic ribbon is wrapped in the two edge sides by organic molecules to form a sandwich structure. The MTT assay result displayed that the synthesised complex possessed antiproliferative activity potentials against the HCT-116, HepG2 and MCF-7 cancer cell lines. After 72 h treatment, the complex had a potent inhibitory effect on HCT-116 cells, and the IC_{50} value was 1.05 ± 0.06 (μg/mL). The cell cycle and apoptosis experiments showed that the complex remarkably induced apoptosis and arrested the HCT-116 cancer cell lines in the G1/G0 phase related to the concentration.
© 2021 The Authors. Published by Elsevier B.V. on behalf of King Saud University. This is an open access article under the CC BY-NC-ND license (http://creativecommons.org/licenses/by-nc-nd/4.0/).

1. Introduction

Heterocyclic compounds with pyrazole group generally have antibacterial, antifungal, anti-inflammatory and enzyme inhibitory effects. Moreover, they possess high efficiency and low toxicity in anti-tumour and anti-virus applications (Liang et al., 2016; Hura et al., 2018). As a pyrazolone derivative, 4-Aminoantipyrine has various biological activities, such as antimicrobial activity, analgesic, antiviral, and can also be used as a precursor for the synthesis of biologically active

* Corresponding authors.
E-mail addresses: 11712010004@stu.bbmc.edu.cn (T. Yin), lwg1010@163.com (W. Li), liangjyt@163.com (L. Liang).
Peer review under responsibility of King Saud University.

Production and hosting by Elsevier

https://doi.org/10.1016/j.arabjc.2021.103117
1878-5352 © 2021 The Authors. Published by Elsevier B.V. on behalf of King Saud University.
This is an open access article under the CC BY-NC-ND license (http://creativecommons.org/licenses/by-nc-nd/4.0/).

compounds (Awad et al., 2007; Burdulene et al., 1999; Evstropov et al., 1992; Raman et al., 2009). Moreover, the recent reports found that 4-Aminoantipyrine had anti-proliferative activity on human cancer cells and as cleavage agents for DNA (Rosu et al., 2010; Raman et al., 2014; Manjunath et al., 2017; Brana et al., 2006; Lin et al., 2007). Studies have shown that 4-Aminoantipyrine combined with anti-tumour drugs adriamycin, cisplatin and cyclophosphamide can reduce its genotoxicity, mutagenesis, apoptosis and phagocytosis (Berno et al., 2016) (see Scheme 1).

It has been proven that certain drugs in the form of metal chelates exhibited higher activity than organic compounds. Cisplatin, as a metal anticancer drug with DNA-targeting properties, it affects many malignancies, such as testicular, ovarian, bladder and breast cancers (Arnesano and Natile, 2009; Santini et al., 2014). However, cisplatin is easy to develop resistance to cancer cells and has significant side effects on human kidneys and nerves (Bruijnincx and Sadler, 2008; Jung and Lippard, 2007). Therefore, further research on novel metallic anticancer drugs with remarkable effect, low side effect and low drug-resistant have become a research hotspot in the field of bio-inorganic chemistry. Cadmium (Cd) is a toxic metal and has toxic effects on many systems in the body, among which liver and kidney are the main target organs (Rao et al., 2009). Cd was identified as a class IA carcinogen (IARC, 1993). It can cause tumours in the lungs, prostate and testicles (Gunn et al., 1963). However, Waalkes et al. discovered the anticancer effect of Cd in the study of cadmium promoting hepatocellular carcinoma in B6C3F1 mice (Waalkes et al., 1991). Other studies also suggested that they gave cadmium to hepatoma mice induced by nitroso diethylamine (NDEA) and found that single dose of Cd could reduce the incidence of liver tumours by 50% and dramatically reduce the diversity of tumors after tumorigenesis (Waalkes et al., 1996). So far, there are few reports of Cd Complexes with anticancer activity. In this paper, we used 4-Aminoantipyrine as the ligand to synthesise the Cd (II) complex $[Cd_7Cl_{14}L_2(EtOH)_2]n$. This complex has an unusual seven-nuclear cadmium chloride structure. The flat inorganic ribbon is wrapped in the two edge sides by organic molecules to form a sandwich structure. This structure could reduce its toxicity, but it still has anticancer activity, especially HCT-116 cancer cell.

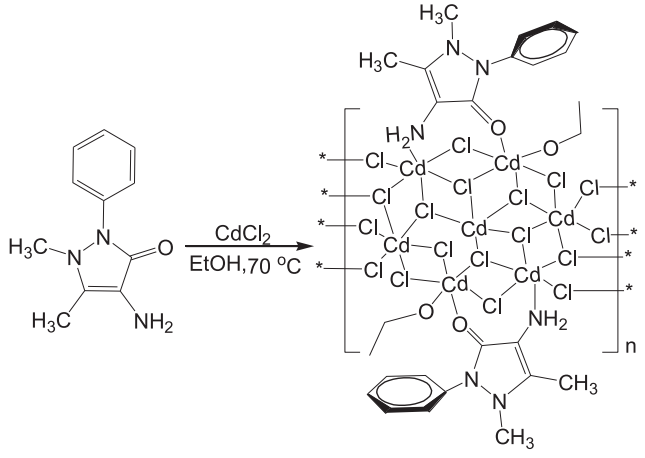

Scheme 1 Synthesis scheme of Cd (II) complex.

2. Materials and instruments

2.1. Synthesis of the complex $[Cd_7Cl_{14}L_2(EtOH)_2]n$

4-Aminoantipyrine (0.0203 g, 0.1 mmol), $CdCl_2{\cdot}2.5H_2O$ (0.142 g, 0.06 mmol), 2 mL ethanol and 6 mL ethyl acetate were mixed and slightly heated (70 °C) for 3 d with stirring. The yellow-green bulk crystals were obtained. The crystals were separated by filtration and washed with ethanol. Infrared (IR) (KBr, cm^{-1}): 3734 (w), 3709 (w), 3627 (w), 3544 (w), 3260 (w), 2356 (s), 2342 (s), 1609 (s), 1557 (s), 1491 (m), 1456 (m), 1324 (m), 1072 (s), 769 (s), 702 (w), 669 (w), 505 (w).

2.2. Structure determination

The single crystal X-ray diffraction data of the complex were measured using a Bruker Smart APEX II diffractometer equipped with graphite monochromatic Mo-Kα radiation (λ = 0.71073 Å). The data were calibrated using SAINT and SADABS software. The structure can be analyzed by a direct method and improved with the Olex2 software package. All non-hydrogen atoms were refined with anisotropic displacement parameters. Hydrogen atoms were generated geometrically and refined by a riding-mode. Detailed crystallographic data and structure refinement parameters are listed in Table 1.

2.3. Antiproliferative assay

Both the human cancer cells (HCT-116, HepG2 and MCF-7 cell lines) and normal human intestinal epithelial cells

Table 1 Crystal data and refinement parameters for the Cd (II) complex.

Items	Cd (II) complex
Formula	$C_{26}H_{38}Cd_7Cl_{14}N_6O_4$
Formula weight	1781.72
Crystal system	Triclinic
Space group	$P\bar{1}$
a/Å	9.9039(6)
b/Å	10.9765(7)
c/Å	12.2519(8)
α/(°)	70.345(2)
β/(°)	88.481(2)
γ/(°)	79.590(2)
Z	1
V/Å^3	1232.81(14)
T/K	173(2)
D_c/(g·cm^{-3})	2.400
F (000)	842
μ/mm^{-1}	3.757
Crystal size/mm^3	0.080 × 0.070 × 0.050
Reflections collected	13910
Independent reflections	4505
R_{int}	0.0830
GOF on F^2	0.991
R_1,wR_2 [all data]	0.1146, 0.0514
R_1,wR_2 [$I > 2\sigma(I)$]	0.0436, 0.0414
Largest diff. peak and hole	0.790 and −0.750 e.Å^{-3}
CCDC No	1936730

(NCM460 cells) were all come from the American Tissue Culture Collection (ATCC, USA). The anti-proliferative activity of the complex was investigated by MTT assay, and 0.1% DMSO was used as a positive control. MCF-7 cells were cultured in DMEM, and HepG2 and HCT-116 cells were cultured in RPMI-1640, and they all contained 10% fetal bovine serum (FBS), 1% penicillin and streptomycin. All cell lines were incubated at 37 °C with 5% CO_2. The cells in the log phase were seeded in a 96-well culture plate at a density of 1×10^5 cells/well. Until 80% cell was fused, cells were incubated for 2 h to synchronise. Discarded the culture supernate, the cancer cells were incubated with the complex (0, 0.625, 1.25, 2.5, 5 and 10 μg/mL, respectively) for 24, 48 and 72 h. Add 20 μL (5 mg/mL) MTT reagent to each well before 4 h of incubation. Use the microplate reader (Berthold LB941, Germany) to measure the absorbance at 570 nm. IC_{50} values were calculated using the percentage of growth versus untreated control. The cytotoxicity of the complex is expressed as the percentage of cell proliferation inhibition.

2.4. Cell apoptosis analysis

Cell apoptosis was determined using KeyGEN Biotech Apoptosis Assay kit (Nanjing, China). Incubated HCT-116 cancer cells (1×10^6/well) in a 6-well plate for 12 h, and then treated them with DMSO and the complex (0, 1, 3 and 10 μg/mL, respectively). After 48 h, harvested the cells and washed three times with ice-cold PBS. A 0.5 mL of staining buffer and 5 μL of FITC were added. The cells were incubated in the dark for 15 min. After staining, 5 μL of PI buffer was added, mixed gently and kept on ice. The samples were tested with Beckman DxFlex flow cytometer.

2.5. Cell cycle analysis

After the HCT-116 cells were cultivated in a 6-well plate for 12 h, they were treated with DMSO and the complex (0, 1, 3 and 10 μg/mL, respectively). The cells were collected at 48 h and fixed with 70% pre-cooled ethanol at 4 °C overnight. Cells were cultivated with about 3 μL of DNase-free RNase (the final concentration was 50 μg/mL) for 30 min and stained by propidium iodide (PI) staining solution (the final concentration was 65 μg/mL) on ice in the dark for 30 min. DNA content was determined by Beckman DxFlex flow cytometer.

3. Results and discussion

3.1. Crystal structure

One-dimensional (1D) cadmium coordination frameworks, $[Cd_7Cl_{14}L_2(EtOH)_2]n$, (L = 4-Aminoantipyrine) was obtained through in situ solvothermal synthesis and structurally characterised by elemental analyses, thermal gravimetric analysis, and single-crystal and powder X-ray diffraction. The crystal data and structure refinement for Cd (II) complex are listed in Table 1.

X-ray crystallographic analysis indicated that complex **1** crystallises was in the triclinic space group $P\bar{1}$ (No. 2). The asymmetric unit contained four crystallographically unique Cd (II) atoms, seven Cl atoms, one ethanol and one unique L ligand (Fig. 1). The occupancy of Cd1 is 1, Cd2, Cd3 and Cd4 are 0.5. The Cd1 atom, sitting on an inversion centre, is coordinated by two Cl1, two Cl2 and two Cl3 atoms. The Cd-Cl distances are 2.5506(19), 2.6408(18) and 2.6446(19) Å. Cl1, Cl2 and Cl3 atoms connect three Cd atoms in a μ_3-bridging mode. Cl4, Cl5 and Cl7 atoms connect two Cd atoms in a μ_2-bridging mode. The molecule structure contains seven Cd (II) atoms, fourteen Cl atoms, two ethanol molecules and two L ligands (Fig. 2). Cd1, Cd2, Cd3 and Cd4 all have an octahedral coordination geometry. Cd1 and Cd2 are coordinated by six Cl atoms. Cd3 is coordinated by five Cl atoms and one nitrogen atom. Cd4 is coordinated by four Cl atoms and two oxygen atoms, one from carbonyl and one from ethanol. Cd1 sitting at a center of inversion is connected to six surrounding Cd atoms by six μ_3-Cl atoms, furnishing a seven-nuclear $[Cd_7Cl_{14}]$ cluster. The six surrounding Cd atoms and the central Cd atom are coplanar, with half Cl atoms up of the plane and half under the plane (Fig. 3). The $[Cd_7Cl_{14}]$ cluster is flower-like and such unit is rare in the reported coordination polymers containing Cd and chlorine atoms.

The flower-like $[Cd_7Cl_{14}]$ cluster is surrounded by two ethanol and two ligands, which is further connected by two Cl4 and two Cl6 atoms to form an infinite flat ribbon $[Cd_7Cl_{14}L_2(EtOH)_2]_n$ (Fig. 4). The width of the ribbon is 18 Å, and the thickness is 3 Å. So the infinite ribbon containing the centre $[Cd_7Cl_{14}]$ cluster is an inorganic ribbon which is

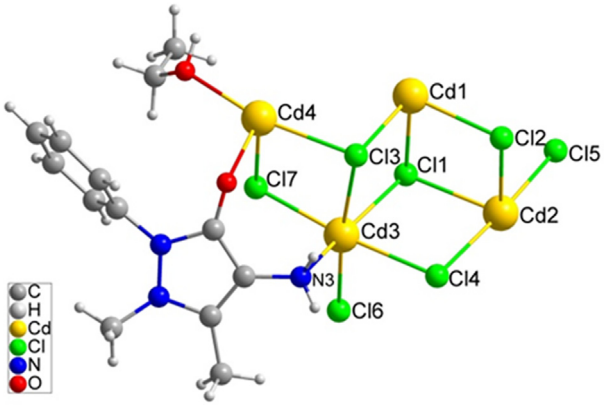

Fig. 1 The asymmetric unit of **1.**

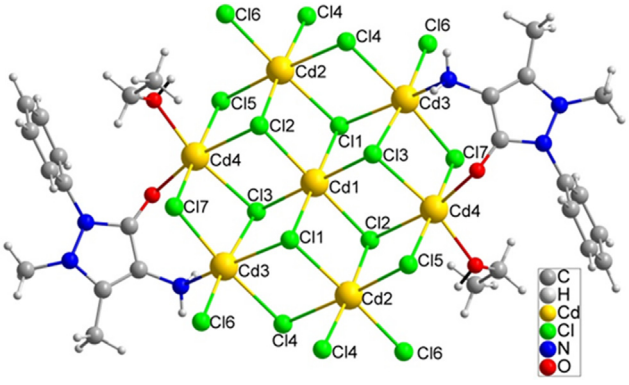

Fig. 2 The molecule structure of the heptanuclear cadmium cluster.

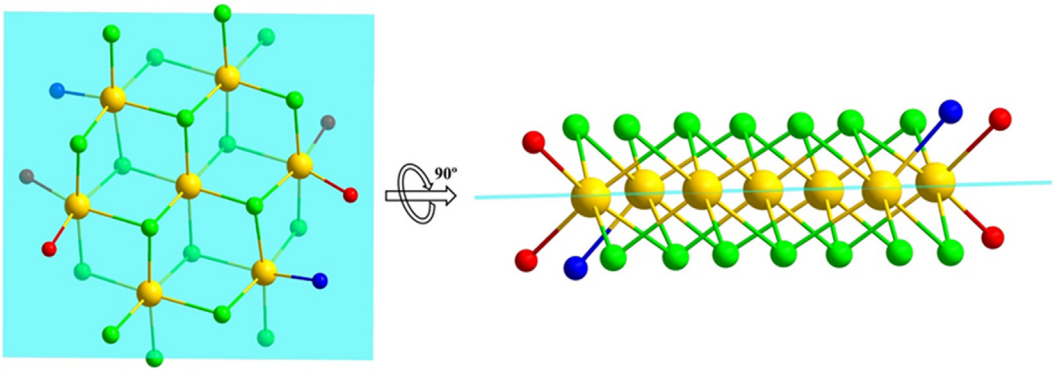

Fig. 3 The seven Cd atoms are coplanar (cyan plane) with half Cl ions up and half under the plane (vertical view and side view).

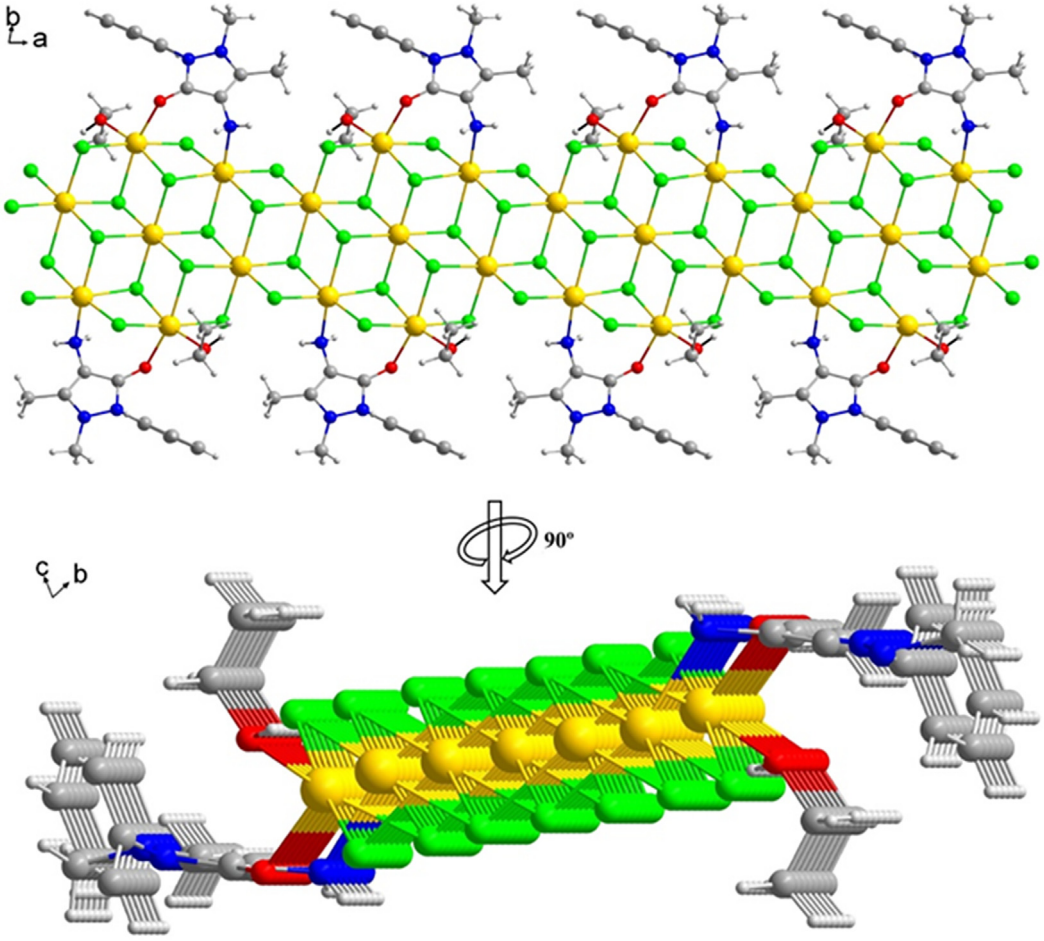

Fig. 4 The 1D ribbon $[Cd_7Cl_{14}L_2(EtOH)_2]n$ extends along the *a*-axis.

surrounded and wrapped in the two edge sides by organic molecules to form sandwich structure (Fig. 5). There are a few kind of cadmium chloride inorganic chains, but such kind of flower-like seven-nuclear ribbon has not been reported (Jiang and Mao, 2006; Zhai et al., 2011; Mobin et al., 2014; Ou et al., 2015; Soudani et al., 2015). As Cd atom is poisonous, the centre Cd atoms are wrapped by Cl atoms on the two faces and organic molecules in the two edge sides. This wrapped inorganic ribbon structure may help to avoid the release of Cd atoms, which may reduce the toxicity of cadmium. The infinite ribbon $[Cd_7Cl_{14}L_2(EtOH)_2]_n$ extends along the *a*-axis, and there are no weak interactions between the chains (Fig. 6).

3.2. Powder X-ray diffraction (PXRD) and electrical conductivity

To confirm the purity of the complex, we carried out the PXRD experiments. The experimental and structure-simulated powder XRD patterns were compared and the

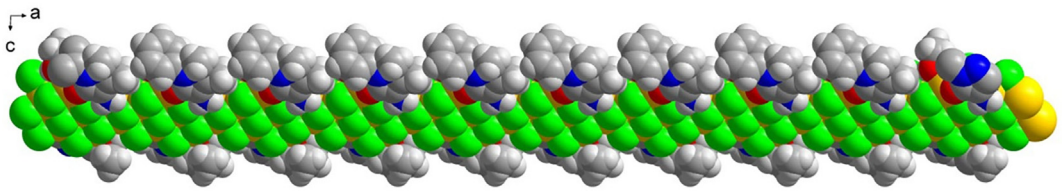

Fig. 5 The sandwich structure of the $[Cd_7Cl_{14}L_2(EtOH)_2]n$ ribbon.

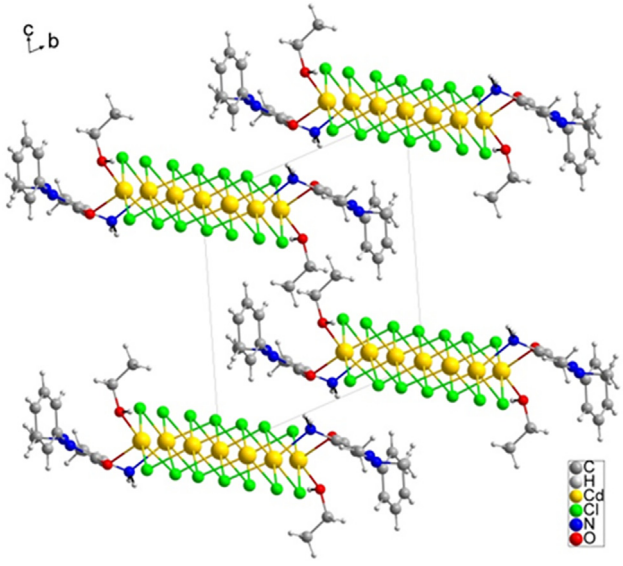

Fig. 6 The $[Cd_7Cl_{14}L_2(EtOH)_2]n$ ribbons are isolated without weak interactions.

results showed that the main peaks of the synthesized bulk materials matched well with the simulated ones, indicating the phase purity (Fig. 7). The title complex is soluble in DMSO, and its solubility in water is small. The powder XRD patterns of the sample after soaked in water are similar with the simulated peaks, indicating the main structure of the sample maintains.

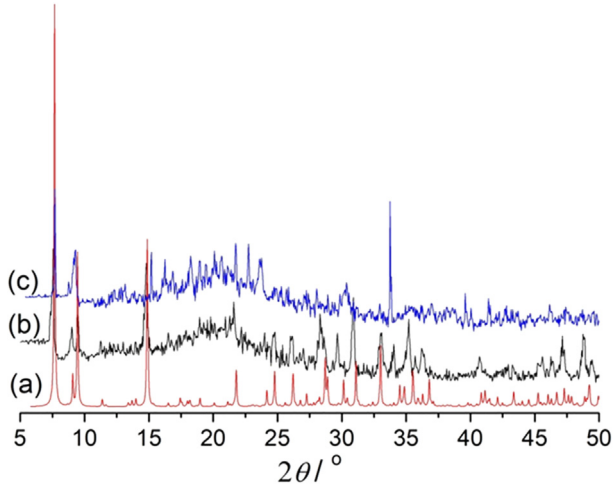

Fig. 7 PXRD pattern of the complex: (a) simulated, (b) synthesized, and (c) after soaked in water.

Table 2 Electrical conductivity values of $CdCl_2$ and the title complex.

Substance	Mass	Solvent	Conductance Value
$CdCl_2$	0.005 g	10 mL H_2O	8.0 mS/cm
	0.005 g	10 mL DMSO/H_2O	3.0 mS/cm
	0.0178 g	10 mL DMSO	1.3 mS/cm
Complex	0.005 g	10 mL H_2O	4.0 mS/cm
	0.005 g	10 mL DMSO/H_2O	1.6 mS/cm
	0.0178 g	10 mL DMSO	0.7 mS/cm

Table 3 Growth inhibition of HepG2, HCT-116, MCF-7 and NCM460 cell lines in different concentrations of the complex after 24, 48 and 72 h incubation (IC_{50} values in μg/mL).

Cell line	IC_{50} (μg/mL)		
	24 h	48 h	72 h
NCM460	30.30 ± 1.76	23.21 ± 1.37	16.44 ± 1.09
HepG2	7.52 ± 0.38	6.38 ± 0.16	5.65 ± 0.16
HCT-116	2.43 ± 0.23	1.69 ± 0.05	1.05 ± 0.06
MCF-7	8.08 ± 0.20	7.24 ± 0.14	6.34 ± 0.07

Note: Cancer Cells were incubated with the complex (0, 0.625, 1.25, 2.5, 5 and 10 μg/mL, respectively) for 24 (A), 48 (B) and 72 h (C). At the same time, the NCM460 cells were incubated with the complex (0, 1, 3, 10, 30 and 100 μg/mL, respectively). Cell viability was determined using MTT assay. Results were mean ± SD for five repeats for each condition.

To further investigate the stability of the title complex in DMSO, the electrical conductivity of the complex was measured. The conductivity values of the complex and cadmium chloride are listed in Table 2. We can see from the table that in 10 mL H_2O, the conductance values of the title complex and $CdCl_2$ are 4.0 and 8.0 mS/cm, respectively, while in 10 mL DMSO/H_2O, the conductance values are 1.6 and 3.0 mS/cm, respectively. The title complex has half conductance values of the $CdCl_2$ in both water and DMSO/H_2O mixing solution. Combined with the PXRD and conductance data, we can reach the conclusion that there could be some chloride ions dissociated from the $[Cd_7Cl_{14}L_2(EtOH)_2]n$ ribbon in DMSO and water solutions, but the primary ribbon structure maintains. (See Table 3.)

3.3. Thermogravimetric analysis (TGA)

In order to estimate the pyrolysis behavior of the complex, the crystal samples were analyzed by TGA and differential

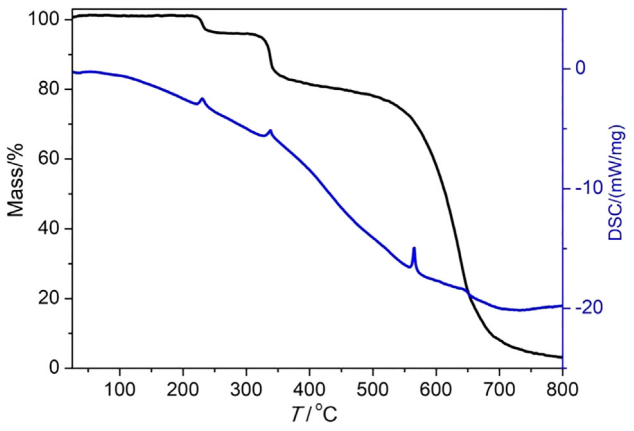

Fig. 8 The TG-DSC curve of the complex.

scanning calorimetry (DSC) under the protection of nitrogen atmosphere. As shown in Fig. 8, thermogravimetric analysis reveals no mass loss under 200 °C. The weight loss with an endothermic peak at 220 °C is 4.83%. The reason may be due to the decomposition of two coordinating ethanol molecules (Calcd. 5.17%). The weight gradually dropped to 13.18% at about 330 °C, accompanied by an endothermic peak. This may be due to the loss of one coordinated L molecule (Calcd. 11.41%). And then a gradual decomposition is followed. The pyrolysis of the whole framework occurs at about 600 °C.

3.4. Biological tests

3.4.1. Antiproliferative assay

The cytotoxicity effect of the complex on three cancer cells and normal NCM460 cells were expressed as inhibition rate values in Tab 3. The results showed that the complex had low toxicity to normal cells, and showed a significant inhibitory effect on HCT-116 cells, and the IC_{50} value was 1.05 ± 0.06 after 72 h of treatment. Our complex has a better inhibitory effect on Human colorectal cancer cells Compared with the schiff based $CdCl_2$ complex ($C_{14}H_{21}N_3O_2$) (Hajrezaie et al., 2015).

3.4.2. Cell apoptosis analysis

In order to further study whether the effective anti-proliferative activity of the target complex was related to the enhancement of cancer cell apoptosis, we performed flow cytometry analysis on the HCT-116 cancer cell line and determined the percentage of apoptotic cells. HCT-116 cells were incubated with different concentrations of target complex. After HCT-116 cells were incubated with the complex (0, 1, 3 and 10 μg/mL, respectively) for 48 h. Cell apoptosis rate was determined by FCM. As shown in Fig. 9, the complex remarkably induced apoptosis of HCT-116 cancer cells in connection with the concentration. The complex induced 16.86%, 27.69 and 30.67% apoptosis of HCT-116 cells at 1 μg/mL, 3 μg/mL and 10 μg/mL, respectively.

3.4.3. Cell cycle analysis

Cell cycle analysis of the complex was investigated in HCT-116 cancer cells. The complex induced HCT-116 cancer cells arrested in the G1/G0 phase related to the concentration. The concentration of 10 μg/mL had the most significant effect ($p < 0.05$, $p < 0.01$).

4. Conclusions

In conclusion, we synthesised the complex $[Cd_7Cl_{14}L_2(EtOH)_2]_n$. The $[Cd_7Cl_{14}]$ cluster is an inorganic ribbon structure

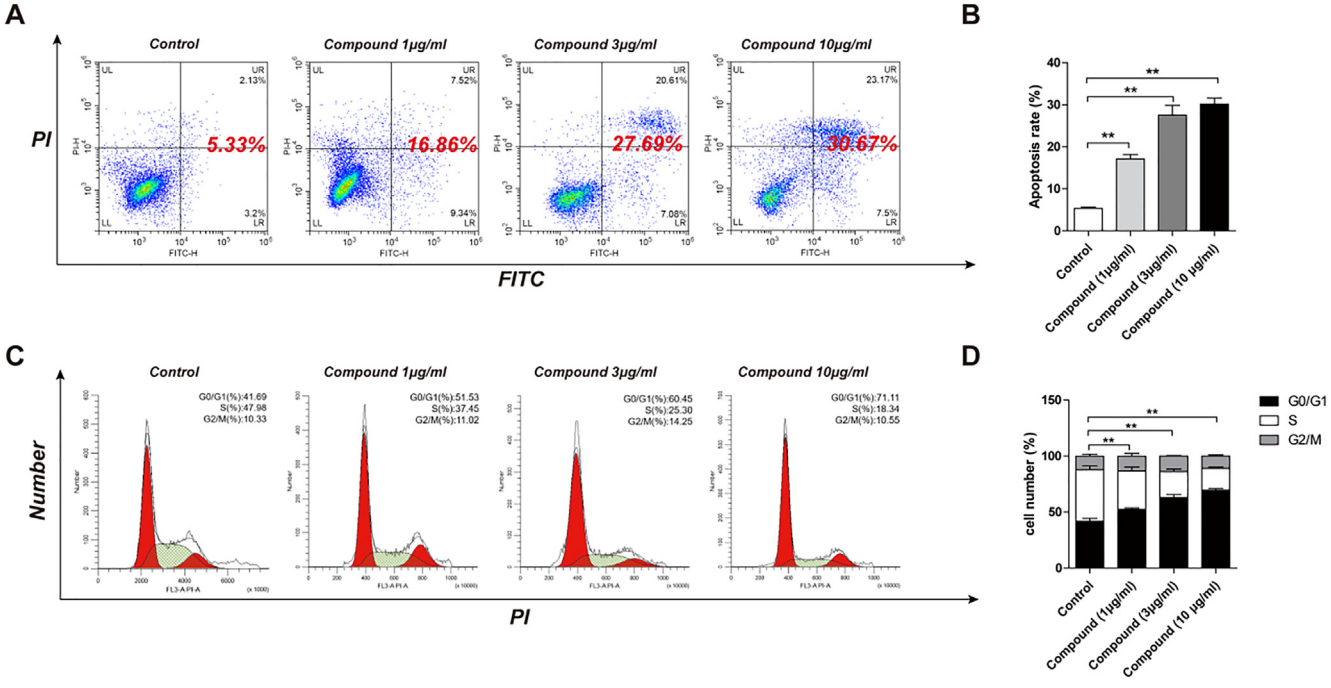

Fig. 9 The effect of the complex on HCT-116 cells cell cycle and cell apoptosis rate. After HCT-116 cells were incubated with the complex (0, 1, 3 and 10 μg/mL, respectively) for 48 h, cell apoptosis rate and cell cycle of HCT-116 cells were determined by FCM. Results were mean ± SD for five repeats for each condition.

wrapped in the two edge sides by organic molecules to form a sandwich structure. The MTT assay results showed the HCT-116 cells had the best inhibitory effect. Therefore, the cell cycle and apoptosis experiments were carried out on the HCT-116 cells. The results showed that the complex remarkably induced apoptosis and arrested the HCT-116 cells in the G1/G0 phase related to the concentration. The experiment results showed that the synthesised small molecular substance had good anticancer activity. The above results provide a theoretical basis for the later research on the mechanism.

Declaration of Competing Interest

The authors declare that they have no known competing financial interests or personal relationships that could have appeared to influence the work reported in this paper.

Acknowledgements

We thank the financial support of Science Foundation of Bengbu Medical College (BYKY1701ZD), the Key Natural Science Research Foundation for University of Anhui (KJ2019A0312), Key Special Project of Transforming Medicine of Bengbu Medical College (BYTM2019001), and the Natural Science Foundation of Anhui Provence (1908085MB45) and 512 Talent Cultivation Foundation of Bengbu Medical College (51201201). We also thank Peipei Zong and Zhenxiang Pan for their chemical synthesis work.

References

Arnesano, F., Natile, G., 2009. Mechanistic insight into the cellular uptake and processing of cisplatin 30 years after its approval by FDA. Coordin. Chem. Rev. 253, 2070–2081. https://doi.org/10.1016/j.ccr.2009.01.028.

Awad, L., Ibrahim, E., Bdeewy, O.K., 2007. Synthesis of antipyrine derivatives derived from dimedone. China J. Chem. 25, 570–573. https://doi.org/10.1002/cjoc.200790107.

Berno, C.R., Barbara, D.T.R., Silveira, I.O.M.F.D., Coelho, H.R., Antoniolli, A.C.M.B., Adilson, B., Dênis, P.D.L., Monreal, A. C.D., Fabricio, G.S., Gomes, R.D.S., Rodrigo, J.O., 2016. 4-Aminoantipyrine reduces toxic and genotoxic effects of doxorubicin, cisplatin, and cyclophosphamide in male mice. Mutation Res. 805, 19–24. https://doi.org/10.1016/j.mrgentox.2016.05.009.

Brana, M.F., Gradillas, A., Ovalles, A.G., Lopez, B., Acero, N., Llinares, F., Mingarro, D.M., 2006. Synthesis and biological activity of N, N-dialkylaminoalkyl-substituted bisindolyl and diphenyl pyrazolone derivatives. Bioorg. Med. Chem. 14, 9–16. https://doi.org/10.1016/j.bmc.2005.09.059.

Bruijnincx, P.C., Sadler, P.J., 2008. New trends for metal complexes with anticancer activity. Curr. Opin. Chem. Biol. 12, 197–206. https://doi.org/10.1016/j.cbpa.2007.11.013.

Burdulene, D., Palaima, A., Stumbryavichyute, Z., Talaikite, Z., 1999. Synthesis and anti-inflammatory activity of 4-aminoantipyrine derivatives of succinamides. Pharm. Chem. J. 33, 191–193. https://doi.org/10.1007/BF02509936.

Evstropov, A.N., Yavorovskaya, V.E., Vorob'ev, E.S., Khudonogova, Z.P., Gritsenko, L.N., Shmidt, E.V., Medvedeva, S.G., Filimonov, V.D., Prishchep, T.P., Saratikov, A.S., 1992. Synthesis and antiviral activity of antipyrine derivatives. Pharm. Chem. J. 26, 426–430. https://doi.org/10.1007/BF00772907.

Gunn, S.A., Gould, T.C., Anderson, W.A.D., 1963. Cadmium-induced interstitial cell tumors in rats and mice and their prevention by zinc. J. Natl. Cancer I. 31, 745–759. https://doi.org/10.1093/jnci/31.4.745.

Hajrezaie, M., Paydar, M., Looi, C.Y., Moghadamtousi, S.Z., Hassandarvish, P., Salga, M.S., Karimian, H., Shams, K., Zahedifard, M., Majid, N.A., Ali, H.M., Abdulla, M.A., 2015. Apoptotic effect of novel schiff based $CdCl_2$ ($C_{14}H_{21}N_3O_2$) complex is mediated via activation of the mitochondrial pathway in colon cancer cells. Sci. Rep. 3, 1–11. https://doi.org/10.1038/srep09097.

Hura, N., Naaz, A., Prassanawar, S.S., Guchhait, S.K., Panda, D., 2018. Drug-clinical agent molecular hybrid: synthesis of diaryl (trifluoromethyl) pyrazoles as Tubulin Targeting Anticancer Agents. ACS Omega 3 (2), 1955–1969. https://doi.org/10.1021/acsomega.7b01784.

IARC, 1993. Beryllium, cadmium, mercury and exposures in the glass industry, Lyon, France.

Jiang, H.L., Mao, J.G., 2006. $[Cd_2(Te_6O_{13})][Cd_2Cl_6]$ and $Cd_7Cl_8(Te_7O_{17})$: Novel tellurium(IV) oxide slabs and unusual cadmium chloride architectures. Inorg. Chem. 45, 717–721. https://doi.org/10.1021/ic051703q.

Jung, Y., Lippard, S.J., 2007. Direct cellular responses to platinum-induced DNA damage. Chem. Rev. 107, 1387–1407. https://doi.org/10.1002/chin.200731270.

Liang, X., Zang, J., Zhu, M.Y., Gao, Q.W., Wang, B.H., Xu, W.F., Zhang, Y.J., 2016. Design, synthesis, and nntitumor evaluation of 4-Amino-(1H)-pyrazole derivatives as JAKs inhibitors. ACS Med. Chem. Lett. 7 (10), 950–955. https://doi.org/10.1021/acsmedchemlett.6b00247.

Lin, R.H., Chiu, G., Yu, Y., Connolly, P.J., Li, S.J., Lu, Y.H., Adams, M., Fuentes-Pesquera, A.G., Emanuel, S.L., Greenberger, L.M., 2007. Design, synthesis, and evaluation of 3,4-disubstituted pyrazole analogues as anti-tumor CDK inhibitors. Bioorg. Med. Chem. Lett. 17, 4557–4561. https://doi.org/10.1016/j.bmcl.2007.05.092.

Manjunath, M., Kulkarni, A.D., Bagihalli, G.B., Malladi, S., Patil, S. A., 2017. Bio-important antipyrine derived Schiff bases and their transition metal complexes: Synthesis, spectroscopic characterization, antimicrobial, anthelmintic and DNA cleavage investigation. J. Mol. Struct. 1127, 314–321. https://doi.org/10.1016/j.molstruc.2016.07.123.

Mobin, S.M., Mishra, V., Chaudhary, A., Rai, D.K., Golov, A.A., Mathur, P., 2014. Acid-driven dimensionality control of Cd(II) complexes: from discrete double open cubane to one- and three-dimensional networks. Cryst. Growth Des. 14, 4124–4137. https://doi.org/10.1021/cg5007346.

Ou, Y.J., Ding, Y.J., Wei, Q., Hong, X.J., Zheng, Z.P., Long, Y.H., Cai, Y.P., Yao, X.D., 2015. A series of temperature-dependent Cd^{II}-complexes containing an important family of N-rich heterocycles from in situ conversion of pyridinetype Schiff base. RSC Adv. 5, 27743–27751. https://doi.org/10.1039/c4ra16198j.

Raman, N., Mitu, L., Sakthivel, A., Pandi, M., 2009. Studies on DNA cleavage and antimicrobial screening of transition metal complexes of 4-aminoantipyrine derivatives of N_2O_2 type. J. Iran Chem. Soc. 6, 738–748. https://doi.org/10.1007/BF03246164.

Raman, N., Sakthivel, A., Pravin, N., 2014. Exploring DNA binding and nucleolytic activity of few 4-aminoantipyrine based amino acid Schiff base complexes: A comparative approach. Spectrochim. Acta Part A Mol. Biomol. Spectrosc. 125, 404–413. https://doi.org/10.1016/j.saa.2014.01.108.

Rao, B.S.S., Sreedevi, M.V., Rao, N.B., 2009. Cytoprotective and antigenotoxic potential of Mangiferin, a glucosylxanthone against cadmium chloride induced toxicity in HepG2 cells. Food Chem. Toxicol 47, 592–600. https://doi.org/10.1016/j.fct.2008.12.017.

Rosu, T., Negoiu, M., Pasculescu, S., Pahontu, E., Poirier, D., Gulea, A., 2010. Metal-based biologically active agents: Synthesis, characterization, antibacterial and antileukemia activity evaluation of Cu(II), V(IV) and Ni(II) complexes with antipyrine-derived compounds. Eur. J. Med. Chem. 45, 774–781. https://doi.org/10.1016/j.ejmech.2009.10.034.

Santini, C., Pellei, M., Gandin, V., Porchia, M., Tisato, F., Marzano, C., 2014. Advances in copper complexes as anticancer agents. Chem. Rev. 114, 815–862. https://doi.org/10.1021/cr400135x.

Soudani, S., Mi, J.X., Lefebvre, F., Jelsch, C., Ben Nasr, C., 2015. Synthesis and physico-chemical studies of a novel layered structure with a heptanuclear Cd complex: $(C_9N_4H_{28})Cd_7(H_2O)_2Cl_{18}\bullet nH_2O$ (n = 5.89). J. Mole. Struc. 1084, 46–54. https://doi.org/10.1016/j.molstruc.2014.12.007.

Waalkes, M.P., Diwan, B.A., Rehm, S., Ward, J.M., Moussa, M., Cherian, M.G., Goyer, R.A., 1996. Down-regulation of metallothionein expression in human and murine hepatocellular tumors: association with the tumor-necrotizing and antineoplastic effects of cadmium in mice. J. Pharmacol. Exp. Ther. 277, 1026–1033. https://doi.org/10.1021/js950493j.

Waalkes, M.P., Diwan, B.A., Weghorst, C.M., Bare, R.M., Ward, J. M., Rice, J.M., 1991. Anticarcin ogenic effects of cadmium in B6C3F1 mouse liver and lung. Toxicol Appl. Pharmacol. 110, 327–335. https://doi.org/10.1016/S0041-008X(05)80015-8.

Zhai, Q.G., Gao, X., Li, S.N., Jiang, Y.C., Hu, M.C., 2011. Solvothermal synthesis, crystal structures and photoluminescence properties of the novel Cd/X/α, ω-bis(benzotriazole)alkane hybrid family (X = Cl, Br and I). Cryst. Eng. Comm. 13, 1602–1616. https://doi.org/10.1039/C0CE00581A.